

11-1970

# Discrete Analysis of a Composite Video Signal

Frank F. Carden

*New Mexico State University - Main Campus*

William P. Osborne

osborne@engr.siu.edu

Alton L. Gilbert

*New Mexico State University - Main Campus*

Follow this and additional works at: [http://opensiuc.lib.siu.edu/ece\\_articles](http://opensiuc.lib.siu.edu/ece_articles)

Published in Carden, F. F., Osborne, W. P., & Gilbert, A. L. (1970). Discrete analysis of a composite video signal. *IEEE Transactions on Broadcast and Television Receivers*, BTR-16(4), 352-374. doi: 10.1109/TBTR1.1970.299512 ©1970 IEEE. Personal use of this material is permitted. However, permission to reprint/republish this material for advertising or promotional purposes or for creating new collective works for resale or redistribution to servers or lists, or to reuse any copyrighted component of this work in other works must be obtained from the IEEE. This material is presented to ensure timely dissemination of scholarly and technical work. Copyright and all rights therein are retained by authors or by other copyright holders. All persons copying this information are expected to adhere to the terms and constraints invoked by each author's copyright. In most cases, these works may not be reposted without the explicit permission of the copyright holder.

## Recommended Citation

Carden, Frank F., Osborne, William P. and Gilbert, Alton L. "Discrete Analysis of a Composite Video Signal." (Nov 1970).

This Article is brought to you for free and open access by the Department of Electrical and Computer Engineering at OpenSIUC. It has been accepted for inclusion in Articles by an authorized administrator of OpenSIUC. For more information, please contact [opensiuc@lib.siu.edu](mailto:opensiuc@lib.siu.edu).

# DISCRETE ANALYSIS OF A COMPOSITE VIDEO SIGNAL

Frank F. Carden, William P. Osborne and Alton L. Gilbert  
Electrical Engineering Department  
New Mexico State University, Las Cruces, New Mexico

## ABSTRACT

In this paper the problem of representing the composite video signal for monochromatic T.V. transmission is examined and a method for computing the required spectral bandwidth is devised suitable for computer applications. The results obtained numerically are compared to measured results and to analytical solutions for a determinate signal for special cases. Comparison is made with some "maximum horizontal resolution" methods with a resulting decrease in bandwidth requirements for most applications.

## INTRODUCTION

A fundamental problem in the design of any communications system is specifying the bandwidth necessary for transmission of the required information. A television system is no different in this respect than any other communication system. However, estimating the bandwidth of a television system is a more complicated problem than its counterpart in most other communication problems. The basic reason for the added complication is that a television system must transmit a two dimensional picture over

---

This work was supported by NASA Grant #NGR-32-003-037. Experimental data furnished by Dickey Arndt, NASA Manned Spacecraft Center, Houston, Texas.

a one dimensional channel.

In most communication problems not only is the bandwidth important but knowledge of the actual spectrum is necessary in order to examine the effects of narrowing this bandwidth. The purpose of this work is to study video spectrums and attempt to answer the question of what is the necessary video bandwidth for satisfactory reproduction and to examine the composite video spectrum. All numerical analysis is based upon the parameters of the Apollo downlink television system but the mathematical developments are for a general television system with only the requirements being that it be monochromatic and use linear scanning for transformation into the time domain.

## PART I

### STANDARD METHODS FOR ESTIMATING VIDEO BANDWIDTH

The vertical resolution of a television system is directly proportional to the number of lines in the scanning pattern. The horizontal resolution is a function only of video bandwidth: i.e., the maximum number of vertical lines which may be reproduced is a function of the bandwidth of the system. It should be observed that the bandwidth necessary to achieve maximum horizontal resolution is not necessarily the bandwidth needed to transmit a given image.

There have been numerous methods devised for estimating the required

video bandwidth of a television system. However, for the purpose of this work, the authors have selected three representative methods which appear most often. All of the methods have two things in common--specifying a worst-case bandwidth which is then used as a design guide-line, and disregarding the actual program material to be transmitted through the system.

#### Method of Maximum Information

One method of determining the bandwidth of a scanned video signal is to assume that each intersection of a vertical line with a horizontal scan line (using the maximum number of vertical lines) is a sample point. This means that the number of sample points will be the product of the number of horizontal scan lines,  $N$ , and the maximum possible number of vertical lines,  $N_h$ . Then each of these sample points may be considered quantized into eight levels. It has been shown that eight quantizing levels will represent an actual analogue television signal with reasonable accuracy. [2]

The channel capacity necessary to transmit any signal is equal to the maximum rate of transmission of information. If  $n$  symbols are assumed to occur with equal probability and each takes an identical time,  $t_t$ , to transmit, then it has been shown [3] that the necessary channel capacity,  $C'$ , is

$$C' = \frac{\log_2 n}{t_t} \text{ bits/sec.} \quad (1)$$

For a television system, the  $n$  symbols become the eight words necessary to represent the amplitude of a sample, and if the eight words are assumed to occur with equal probability, then Equation 1 is applicable to such a system and the channel capacity of such a television system is given by Equation 2.

$$C' = \frac{3}{t_t} \text{ bits/sec.} \quad (2)$$

Now the time required to transmit each sample is the number of samples divided into the vertical framing period

$$t_t = \frac{1}{f_f N N_h} \text{ sec.} \quad (3)$$

Thus the channel capacity required to transmit the assumed signal is

$$C' = 3f_f N N_h \text{ bits/sec.} \quad (4)$$

The appropriate relationship between bandwidth and channel capacity in a noisy channel has been shown to be [4]

$$C' = BW \log_2 \left(1 + \frac{S}{N}\right) \text{ bits/sec.} \quad (5)$$

The signal to noise ratio for high quality image reproduction has been shown to be approximately thirty. [5] Substituting this value and Equation 4 into Equation 5 and rearranging, yields a system bandwidth of

$$BW = .6f_f N N_h \text{ hz.} \quad (6)$$

Using the parameters from Table 1 in Equation 6, an approximation to necessary bandwidth for the Apollo system is obtained as

$$\begin{aligned} BW (\text{mode 1}) &= (.6)(10)(312)(250) \\ &= 468 \text{ khz.} \\ BW (\text{mode 2}) &= (.6)(.625)(500)(1248) \\ &= 247 \text{ khz.} \end{aligned}$$

#### Method of Vertical Bars

In using this method for determining the required system bandwidth, an image consisting of nothing but vertical bars of alternating black and white illumination is assumed. It is further assumed

TABLE I

BASIC SCANNING PARAMETERS OF APOLLO TELEVISION SYSTEM [1]

<u>Parameter</u>	<u>Mode 1</u>	<u>Mode 2</u>
Peak-to-Peak Video Signal	2.4 V	2.4 V
Peak-to-Peak Sync Signal	2.4 V	2.4 V
Horizontal Line Period	312.5 $\mu$ sec	1250 $\mu$ sec
Horizontal Line Frequency	3.2 khz	800 hz
Vertical Framing Period	100 msec	1.6 sec
Vertical Framing Frequency	10 hz	.625 hz
Horizontal Sync Burst Period	30 $\mu$ sec	120 $\mu$ sec
Serrated Vertical Sync Period	2.5 msec	10 msec
Width of Serrations	45 $\mu$ sec	180 $\mu$ sec
Burst Frequency	409.5 khz	409.5 khz
Burst Waveform	Keyed Sinewave	Keyed Sinewave
Number of Lines Per Frame	320	1280
Horizontal Resolution	250 Lines	500 Lines

that these bars are of width  $h/N_h$  where  $h$  is the horizontal width of the picture. Thus the system is being required to operate at its maximum horizontal resolution.

When this type of image is scanned, the ideal video output is a square wave with a period of  $2t_\ell/N_h$  and a fifty percent duty cycle. The assumption is then made that for the purposes of reproduction, a sinewave of this period is sufficient. [6]

Thus, the required bandwidth based on this type of analysis is given by

$$BW = \frac{N_h}{2t_\ell} \text{ hz.} \quad (7)$$

The necessary bandwidth for the Apollo television may be calculated using Equation 7 and parameters from Table 1.

$$BW \text{ (mode 1)} = \frac{210}{2(282.5) \cdot 10^{-6}} = 380 \text{ khz.}$$

$$BW \text{ (mode 2)} = \frac{500}{2(1220) \cdot 10^{-6}} = 205 \text{ khz.}$$

Method of Maximum Rise Time

The output of the scanning transducer when it crosses a vertical black to white boundary is in the ideal case a step function. However, in a real system with finite bandwidth, this step has a rise time which is a function of system bandwidth.

If we assume such a boundary exists, then it follows that the rise time must be less than half the width of one of

the minimum width vertical lines used to specify horizontal resolution. The maximum rise time,  $t_p$ , based on the above discussion becomes

$$t_p = (1/2) \frac{t_\ell}{N_h} \text{ secs.} \quad (8)$$

The upper 3db frequency,  $f_2$ , of a system which will pass a pulse with such a rise time is given by the approximation below which may be found in most texts on video amplifiers. [7]

$$f_2 = \frac{.35}{t_p} \text{ hz.} \quad (9)$$

Since the upper 3db frequency is a close approximation to the required bandwidth, Equations 8 and 9 may be combined to yield an expression for the required system bandwidth.

$$BW = \frac{.7N_h}{t_\ell} \text{ hz.} \quad (10)$$

By making use of Equation 10 and the parameters in Table 1, the bandwidth requirements for the Apollo system may be calculated under these assumptions.

$$BW \text{ (mode 1)} = \frac{(.7)(210)}{282.5 \cdot 10^{-6}} = 521 \text{ khz.}$$

$$BW \text{ (mode 2)} = \frac{(.7)(500)}{1250 \cdot 10^{-6}} = 280 \text{ khz.}$$

## PART II

### THE COMPOSITE VIDEO SPECTRUM

The video signal produced at the output of a camera, using linear scanning, may be expressed as the sum of two signals--the total video signal,  $v(t)$ , and the synchronization signal,  $s(t)$ . The total video signal,  $v(t)$ , may be expressed as the product of three other

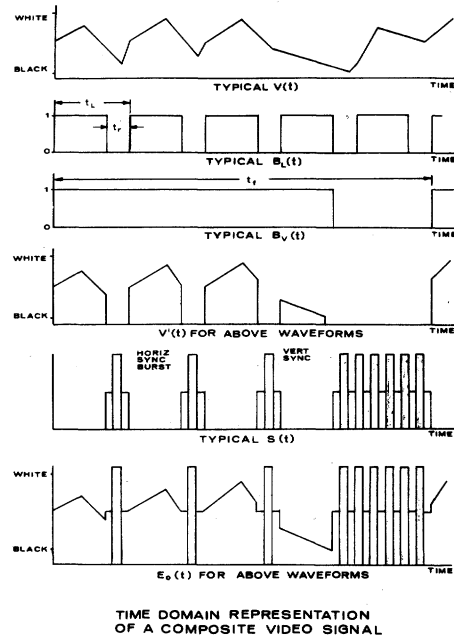


Figure 1

functions. One of these is a video signal,  $v(t)$ , which results from allowing the output of the camera to exist at all times including retrace, or equivalently scanning  $N$  pictures placed side by side with no synchronization or retrace interval involved. The second signal is a blanking signal,  $B_\ell(t)$ , which is zero during horizontal retrace and one at all other times. The third is another blanking signal,  $B_V(t)$ , which is zero during vertical retrace and one at all other times. Thus

$$E_o(t) = V(t) B_\ell(t) B_V(t) + s(t) \quad (11)$$

This argument is illustrated graphically in Figure 1.

Equation 11 has appeared in an article by L. E. Franks on a random video process, but apparently has not been applied to a deterministic video signal before. [9]

### Development of the Composite Video Spectrum Based on a Time Series Model

Using Equation 11 as a starting point, the composite video spectrum may

now be developed. The blanking function,  $B_V$ , represents a square wave with a very high duty cycle and narrow spectrum and, for that reason, neglecting this function has no significant effect on the spectrum of  $E_O(t)$ . [10] Making use of this approximation, Equation 11 becomes

$$E_O(t) = v(t) B_\ell(t) + s(t) \quad (12)$$

$E_O(t)$  is the time representation of the composite video signal as it occurs at the output of the camera, and, therefore, its spectrum is the spectrum to which the remainder of the television system must respond. The spectrum of  $E_O(t)$  is given by the two-sided Fourier transform of  $E_O(t)$ .

$$E_O(\omega) = \int_{-\infty}^{\infty} v(t) B_\ell(t) e^{-j\omega t} dt + \int_{-\infty}^{\infty} s(t) e^{-j\omega t} dt \quad (13)$$

The second integral is the Fourier transform of the synchronization signal or simply  $S(\omega)$ . Equation 13 then becomes

$$E_O(\omega) = \int_{-\infty}^{\infty} v(t) B_\ell(t) e^{-j\omega t} dt + S(\omega). \quad (14)$$

Then  $V'(\omega)$  is given by

$$V'(\omega) = \int_{-\infty}^{\infty} v(t) B_\ell(t) e^{-j\omega t} dt \quad (15)$$

But  $B_\ell(t)$  is periodic and may therefore be represented by a Fourier series. Making use of this fact and rearranging reduces Equation 15 to

$$V'(\omega) = \sum_{n=-\infty}^{\infty} B_\ell(n) \int_{-\infty}^{\infty} v(t) e^{-j(\omega-n\omega_\ell)t} dt \quad (16)$$

$$\text{Where } B_\ell(n) = \frac{1}{t_\ell} \int_0^{t_\ell} B(t) e^{-jn\omega_\ell t} dt$$

$$\text{And } \omega_\ell = 2\pi f_\ell.$$

Making use of the fact that the integral represents another Fourier transform.

$$V'(\omega) = \sum_{n=-\infty}^{\infty} B_\ell(n) v(\omega-n\omega_\ell) \quad (17)$$

Where

$$v(\omega-n\omega_\ell) = \int_{-\infty}^{\infty} v(t) e^{j\omega t} dt \Big|_{\omega=\omega-n\omega_\ell}$$

Equation 17 represents the envelope of the spectrum of the composite video signal.

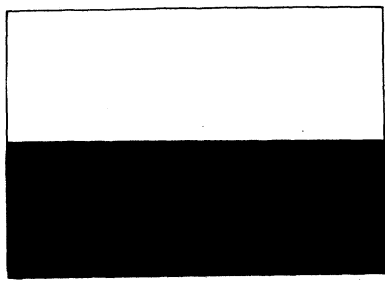
#### Application of this Model to a Black and White Pattern

In order to apply Equation 18 to a black and white test pattern, the Fourier transform of  $v(t)$  and  $B_\ell(t)$  must be obtained. In figure 2, the black and white test pattern is shown with the corresponding  $v(t)$  which it produces. The  $v(t)$  is a square wave of fifty percent duty cycle with its period equal to  $t_f$ . The corresponding  $v(m)$  is known to be

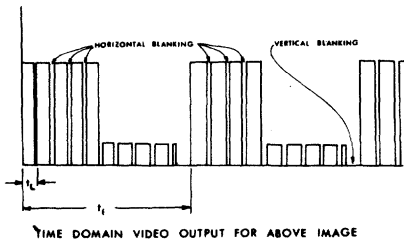
$$v(m) = \frac{t_f}{m\pi} e^{-jm\pi/2} \sin \frac{m\pi}{2}$$

The absolute value of this function is

$$|v(m)| = \left| \frac{t_f}{2} \frac{(\sin \frac{m\pi}{2})}{\frac{\pi}{2}} \right| \quad (18)$$



BLACK AND WHITE TEST PATTERN



BLACK AND WHITE PATTERN

Figure 2

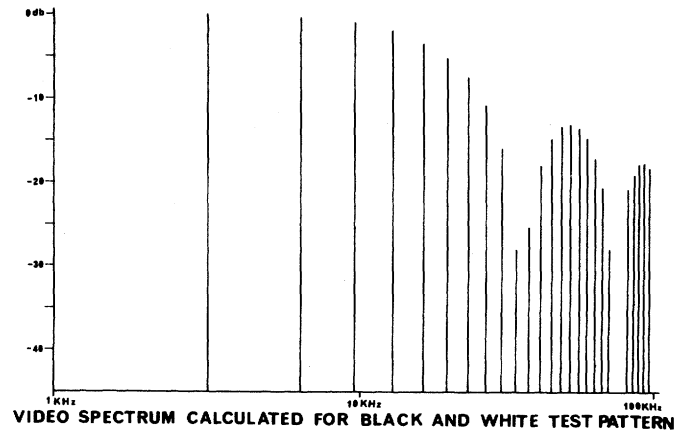
The transform of the blanking signal in Figure 1 is

$$B_{\ell}(n) = \tau e^{-jn\pi\tau/t_{\ell}} \frac{(\sin\pi n\tau/t_{\ell})}{\pi n\tau/t_{\ell}}$$

The absolute value of this function is

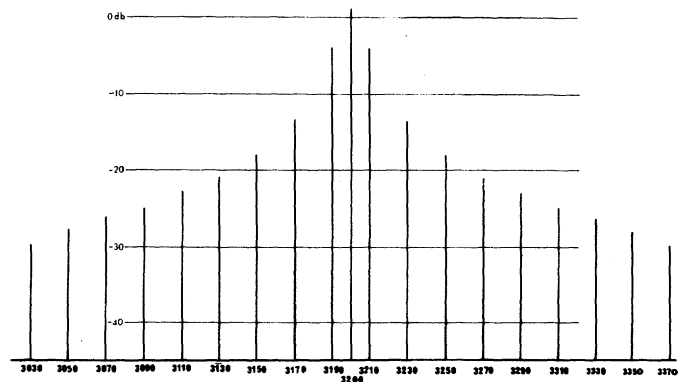
$$|B_{\ell}(n)| = \left| \frac{\tau \sin \frac{n\pi\tau}{t_{\ell}}}{\frac{n\pi\tau}{t_{\ell}}} \right| \quad (19)$$

A plot of the product of Equations 18 and 19 versus frequency is the amplitude spectrum of the composite video signal produced by the black and white pattern. This plot is shown in Figure 3 with the amplitude component of the zero frequency term taken as a zero decibel reference. This plot does not show the components about the line frequency harmonics, because such detail is impossible to achieve on the frequency scale used. However, this detail has been plotted on a linear scale for the first two harmonics and is shown in Figure 4. In making the plot in Figure 3, the values for  $\tau$ ,  $t_{\ell}$ , and  $t_f$  were taken from Table 1 and



VIDEO SPECTRUM CALCULATED FOR BLACK AND WHITE TEST PATTERN

Figure 3



SPECTRUM OF BLACK AND WHITE TEST PATTERN ABOUT THE LINE SCANNING FREQUENCY

Figure 4

correspond to those used in the Apollo television system.

This spectrum was measured by engineers at the Man Space Flight Center in Houston, Texas. Table II is a comparison of the calculated amplitude spectrum with the measured spectrum for the first twenty-eight harmonics. The agreement between the calculated and measured spectrum is quite good with the average difference being less than 2db, and only four components showing greater than 3db error.

The basic video signal,  $v(t)$ , was a ten cycle square wave, yet due to the effect of the blanking signal, this pattern produces components which are only about 40db down from the maximum component at 100khz. This spectrum is analogous to, but certainly not the same as, the spectrum generated by sampling a bandlimited function.

TABLE II

COMPARISON OF CALCULATED RESULTS WITH EXPERIMENT DATA FOR BLACK AND WHITE PATTERN

Line frequency Harmonic number N	Actual Frequency in KHZ	Calculated Amplitude in db	Amplitude Measured by NASA	Difference
1	3.2	-.12	-.4	.28
2	6.4	-.52	-1.5	.98
3	9.6	-1.14	-2.5	1.36
4	12.8	-2.2	-1.0	1.2
5	16.0	-3.6	-2.5	1.1
6	19.2	-5.36	-4.9	.46
7	22.4	-7.72	-6	1.12
8	25.6	-11.04	-7.5	3.5
9	28.8	-16.08	-10	6.08
10	32.0	-28	-12.5	15.5
11	35.2	-25.56	-13.5	12.06
12	38.6	-18.08	-12.5	5.58
13	41.8	-14.88	-12	2.88
14	45.0	-13.56	-11.7	1.8
15	48.2	-13.24	-13.8	.6
16	51.4	-13.68	-14	.32
17	54.6	-14.88	-16	1.22
18	57.8	-17.2	-17.7	.5
19	60.0	-20.92	-20	.98
20	63.2	-28	-23	5.
21	66.4	-48	not present	--
22	69.6	-26	-22	4.
23	72.8	-20.92	-21	.08
24	75.0	-19.2	-19	.2
25	78.2	-18	-17.6	.4
26	81.4	-17.8	-17	.8
27	84.6	-18.56	-19	.44
28	87.8	-20.06	-20	.06



An examination of Equations 18 and 19 reveals some of the parameters which affect this spectrum. From Equation 19, it can be seen that  $B_{\ell}(n)$  has an overall distribution of the familiar  $\sin x/x$  form and that the parameter which controls the width of the spectrum of  $B_{\ell}(n)$  is  $\tau/t_{\ell}$ , the fraction of time spent for retrace.

From Equation 18, the parameters effecting  $v(m)$  may be examined.  $v(m)$  also has a  $\sin x/x$  distribution and its first zero is given by the reciprocal of the pulse width or the reciprocal of the time interval during which the image is white. For this very special case, this time is  $t_f/2$ , thus yielding a spectrum of  $v(t)$  which is approximately 140 cycles wide. If the transition from black to white had been more gradual going through several shades of gray in between, then  $v(t)$  would have had an even narrower spectrum and the frequency components of the composite video would have been much more tightly bound to the harmonics of the line frequency. In the limiting case of a single sine variation from black to white, there would have been only one sideband component for each line frequency harmonic; and it would have been at the framing frequency, 10hz.

Changing the test pattern will have no effect on  $B_{\ell}(n)$ , since it is a function of the scanning parameters. The effect on  $v(m)$ , however, may be quite drastic, since  $v(t)$  is a function of the picture and of the scanning rates.

In considering the effect of other images on the spectrum of  $v(t)$  and thus on the composite video spectrum, it is most helpful to divide the possible  $v(t)$ 's into two classes. The first class will be defined as a set of possible images which will generate a corresponding set of  $v(t)$ 's bandlimited to the bandwidth of  $B_{\ell}(n)$ , the second as a set of possible images which will generate corresponding  $v(t)$ 's which have bandwidths in excess of the bandwidth of  $B_{\ell}(n)$ . In the case of the Apollo system operating in mode one, this dividing bandwidth for the  $v(t)$ 's can be taken as approximately 32 khz. (The first zero of the  $\sin x/x$  distribution describing

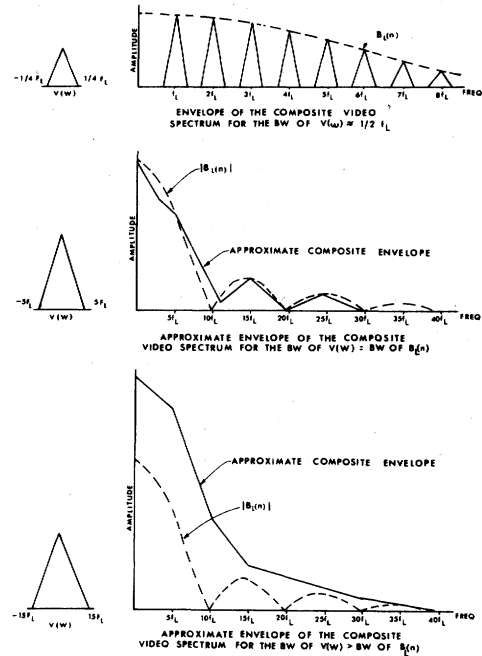


Figure 5

the spectrum of  $B_{\ell}(t)$ ).

For the class of video functions with their bandwidths limited to the bandwidth of  $B_{\ell}(t)$ , the general shape of the spectrum is defined by  $B_{\ell}(n)$ . The justification for this statement can best be shown graphically, but before proceeding to such an argument, consider a restricted case of this class of  $v(t)$ 's. The case is one where  $v(t)$  is bandlimited to less than one-half of the line frequency. For such a situation, the composite video spectrum is given by Equation 17. An example of such a case is plotted in Figure 5a. An inspection of this figure reveals that the bandwidth of the composite video spectrum is given by the bandwidth of the blanking signal.

As the bandwidth of  $v(t)$  is allowed to increase, the situation becomes more complicated, due to the overlapping of the spectrum of  $v(t)$  about each of the line frequency harmonics. An example of this case is shown graphically in Figure 5b. This figure is drawn by considering only five of thirty or forty  $v(w)$ 's displaced about each of the thirty or forty line harmonics given by  $B_{\ell}(n)$ .  $v(w)$  is

placed about each line harmonic with the amplitude of  $v(\omega)$  multiplied by the value of  $B_\ell(n)$  at that harmonic then the envelope of the composite video spectrum was approximated by adding on a point to point basis the envelope of all the  $v(\omega)$ 's. Since only five  $v(\omega)$ 's were considered, this is a fairly crude approximation, but it serves to illustrate the point. A close inspection of Figure 5 will reveal that the harmonics in the upper frequency regions are still very small and that the bandwidth of the composite video signal is still quite close to that of  $B_\ell(t)$  taken alone. However, the actual fine structure of the composite video signal is no longer easily obtained by this method, since it requires adding all of the components of the various overlapping  $v(\omega)$ 's at a frequency to obtain the amplitude of that frequency component. Since the line frequency is a harmonic of the frame frequency and each of the sideband components is separated from the line frequency by multiples of the frame frequency, the overlapping about the line frequency harmonics places sideband components of one line frequency harmonic on top of the sideband components of the next line frequency harmonic.

When the second class of  $v(t)$ 's is present,  $v(t)$  will be the function which determines the bandwidth and not  $B_\ell(t)$ . Consider first the trivial case of  $v(t)$  being a unit impulse. Since  $v(\omega)$  is then displaced about each of the line frequencies, it is obvious that the bandwidth of such a spectrum is infinite, because the  $v(\omega)$  placed about the origin extends to infinity with unity amplitude and the other spectrums are only added to this one.

As a second example, consider a  $v(\omega)$  bandlimited to about four times the bandwidth of  $B_\ell(t)$ , and assume  $v(\omega)$  is a unity constant out to the limiting frequency. A plot of this situation is shown in Figure 5c, once again using only five of the components to obtain the envelope of the spectrum of the composite video. Inspection reveals that the 3db bandwidth of the composite video for this case is given exactly by the bandwidth of

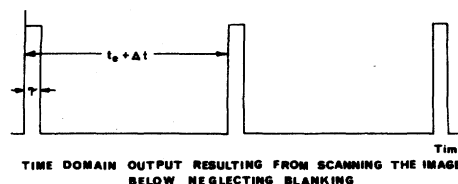
$v(\omega)$ , and the only effect which blanking has on the composite video spectrum is to raise the level of the very high frequency terms, but they still do not become of appreciable size.

It should be pointed out that the division between the two classes of  $v(t)$ 's is somewhat arbitrary. If either  $v(t)$  or  $B_\ell(t)$  has high frequency components compared to the other, it will define the bandwidth of the system. For the intermediate cases, the bandwidth is greater than either  $v(t)$  or  $B_\ell(t)$  would indicate, but no simple approximation can be used to find the bandwidth in this case.

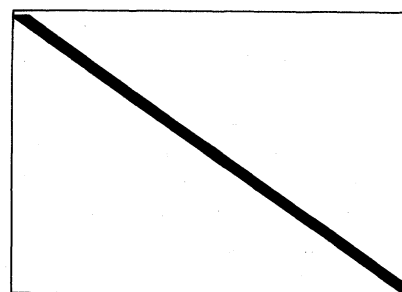
#### Determination of a More Complicated $v(t)$

As a final example, consider the video function,  $v(t)$  generated by scanning a white diagonal bar on a black background. The optical image and the corresponding time domain output of the scanning device are shown in Figure 6.

$v(t)$  consists of a series of pulses each of width  $\tau$  and each periodic at the framing frequency. The spectrum of any one of the periodic pulse trains is given by the Fourier series expansion of the pulse train. Denoting this expansion as  $K_1(t)$ , the series becomes



TIME DOMAIN OUTPUT RESULTING FROM SCANNING THE IMAGE BELOW NEGLECTING BLANKING



DIAGONAL BAR IMAGE

DIAGONAL BAR EXAMPLE

Figure 6

$$K_1(t) = \sum_{n=-\infty}^{\infty} K_1(n) e^{jn\omega_f t} \quad (20)$$

$$\text{Where } K_1(n) = \frac{1}{t_f} \int_0^{t_f} K_1(t) e^{-jn\omega_f t} dt$$

$$\text{and } \omega_f = 2\pi f_f$$

Thus carrying out the indicated integration for the pulse train in question,

$$K_1(n) = \tau e^{-jn\omega_f \tau} \frac{(\sin n\omega_f \pi \tau / 2)}{n\omega_f \pi \tau / 2} \quad (21)$$

Thus the envelope of  $K_1(t)$  is given by the familiar  $\sin x/x$  distribution with the first zero occurring when  $\omega = 1/\tau$ .

However, the spectrum of  $v(t)$  is given by a summation of  $\ell$  such pulse trains or

$$v(t) = \sum_{i=0}^{\ell} K_i(t) \quad (22)$$

By substituting Equation 20 into Equation 22, the Fourier series representation of  $v(t)$  becomes

$$V(t) = \sum_{i=0}^{\ell} \sum_{n=-\infty}^{\infty} K_i(n) e^{jn\omega_f t} \quad (23)$$

An inspection of Equation 23 reveals that the summing of these pulse trains affects only the amplitude of the components. Thus for some fixed  $n$ , say  $n_1$ , it is necessary to sum all of the  $K_i$ 's from each train of pulses to find the amplitude of the component at  $n_1$ . But for some fixed  $n$ , the amplitude of all the  $K$ 's is the same and the only difference in the  $K$ 's is the phase of the components. This phase difference is caused

by the fact that the beginning on one pulse train is delayed by one line scan period (plus  $\Delta t$  due to the slant of the line) from the preceding pulse train. Thus, the phase shift  $\theta$  as function of the time delay,  $t_d$ , between pulses is given by

$$\theta = 2\pi t_d f \quad (24)$$

Where  $f$  is the frequency of the component in question.

The time delay,  $t_d$ , between the first and second pulses is  $t_\ell + \Delta t$ ; and between the first and third, it is twice this much or, in general for the  $i^{\text{th}}$  pulse, it is  $i(t_\ell + \Delta t)$ . The amplitude of the  $n_1$  component,  $A(n_1)$ , may be now expressed as the sum of terms with identical amplitudes and phases given by Equation 24 or

$$\begin{aligned} A(n_1) &= K_1(n_1) + K_2(n_1) e^{j2\pi t_d f} \\ &+ K_3(n_1) e^{j4\pi t_d f} + \dots \\ &+ K_\ell(n_1) e^{j2\pi \ell t_d f} \end{aligned}$$

However, by recalling the  $K_1(n_1) = K_2(n_1) = \dots = K_\ell(n_1)$  the expression reduces to

$$A(n_1) = K(n_1) \sum_{i=0}^{\ell} e^{j2\pi i T f} \quad (25)$$

Where  $T = t_\ell + \Delta t$

However, the series in Equation 25 may be put into closed form [10], and the results are

$$\sum_{i=0}^{\ell} e^{j2\pi i T f} = \frac{\sin \pi \ell T f}{\sin \pi T f} \quad (26)$$

Substitution of Equation 26 into Equation 25 yields an expression for  $A(n_1)$ .

$$A(n_1) = \left| K(n_1) \frac{\sin \pi \lambda T f}{\sin \pi T f} \right| \quad (27)$$

Since Equation 27 is good for any fixed  $n$ , it may be substituted into Equation 23 to obtain the Fourier series representation of  $v(t)$  as

$$v(t) = \sum_{n=-\infty}^{\infty} K(n) \frac{\sin \pi \lambda T n f}{\sin \pi T n f} e^{jn\omega_f t} \quad (28)$$

The envelope of the resulting  $v(t)$  has been plotted in Figure 7 assuming a vertical line; i.e.,  $\Delta t = 0$ . The effect of having the sum of pulse trains instead of only one pulse train is to modulate the envelope of  $K(n)$  with

$$\frac{\sin \pi \lambda T n f}{\sin \pi T n f}$$

The main effect of this modulation is to concentrate the energy in bands about the harmonics of the line frequency. Observe that this concentration is accomplished without consideration of the blanking frequency, and that when the pulse width is small, the effect of the blanking signal on the composite video spectrum is very minor by the arguments presented in the last section. Thus, in this case, the bandwidth necessary to transmit the composite video signal is determined by the  $v(t)$  and, more specifically, by the  $\sin x/x$  envelope of one of the pulses.

One last point of interest is what happens when  $\Delta t$  is not zero: i.e., when the line is rotated. Examination of the modulating function will reveal that it is periodic and has peaks located at  $f = 1/T$ . Therefore, if  $\Delta t$  is not zero, then the peaks of the spectrum envelope occur at  $f = 1/t_\ell + \Delta t$  and harmonics of  $f$ . Thus, for a  $\Delta t$  small, in comparison with  $t_\ell$ , the first peak is very near the line frequency, but for the higher

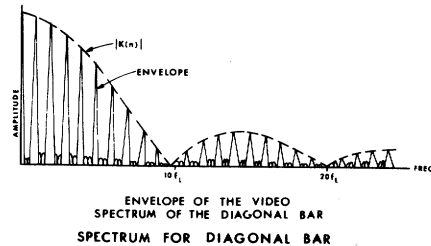
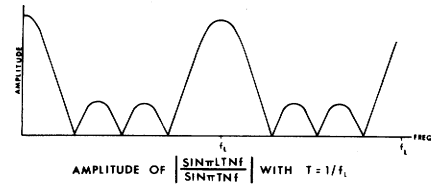
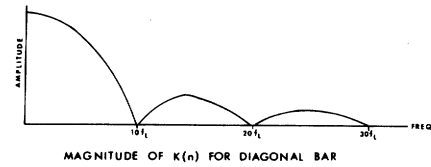


Figure 7

harmonics of  $f$ , the peak occurs farther away from the line frequency and thus the spectrum becomes more diffused in the higher portion of the video range for non-vertical lines.

This effect is analogous to putting a band of frequencies into a frequency doubling circuit, and the output is a band of frequencies twice as wide. For example, if  $\Delta t$  is  $.01t_\ell$ , then the first peak occurs at  $f = .99f_\ell$ , but the 50th peak occurs at  $f = 49.5f_\ell$  or halfway between the forty-ninth and fiftieth harmonic of the line frequency.

### PART III

#### GENERAL METHOD FOR OBTAINING THE SPECTRUM OF THE VIDEO SIGNAL

In Part II, a mathematical model of the composite video signal was presented, but in order to use this model, it is necessary to evaluate the function  $v(t)$ . This function may be obtained by performing the scanning process mentally and thus generating the video signal, as was done for the previous two examples. This process, however, becomes very complicated for a picture of any complexity. It is therefore of interest to have a

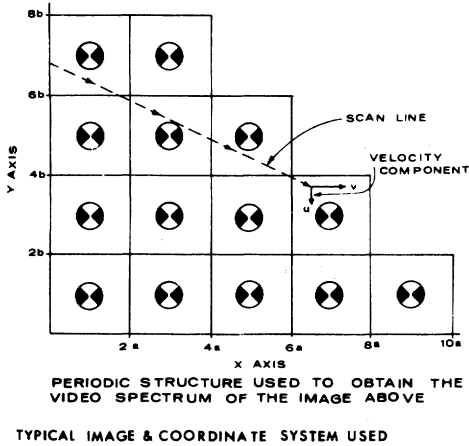
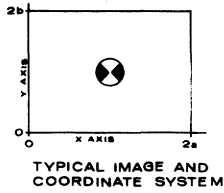


Figure 8

method for obtaining the spectrum of  $v(t)$  directly from the image and thus avoid the step of transformation into the time domain. In this section, a method developed by P. Mertz and F. Gray [11] for obtaining the spectrum of  $v(t)$  directly will be summarized and a numerical technique for machine computation based on this method will be developed.

### Harmonic Analysis of Scanned Optical Images

Figure 8 represents a typical image to be transmitted through a television system. The brightness function over the surface is defined as  $B(x,y)$ .

Now Mertz and Gray [11] have shown that

$$B(x,y) = \sum_{k=-\infty}^{\infty} \sum_{\ell=-\infty}^{\infty} C_{k\ell} e^{j \left( \frac{\pi k}{a} x + \frac{\pi \ell}{b} y \right)} \quad (29)$$

And that

$$v(t) = A_g \sum_{k=0}^{\infty} \sum_{\ell=-\infty}^{\infty}$$

$$A_{k\ell} \cos \left[ \pi \left( \frac{kv}{a} + \frac{\ell u}{b} \right) t + \phi_{k\ell} \right] \quad (30)$$

Where

$A_g$  = conversion gain of the scanning device

$v$  = velocity of the scanning device in the x direction

$u$  = velocity of the scanning device in the y direction

$$A_{k\ell} = \frac{1}{2} C_{k\ell} e^{j\phi_{k\ell}}$$

$$A_{-k,-\ell} = \frac{1}{2} C_{k\ell} e^{-j\phi_{k\ell}}$$

Now recalling that  $v/a = 2/t_\ell$  and  $u/b = 2/t_f$  and taking  $A_g = 1$  for convenience

$$v(t) = \sum_{k=0}^{\infty} \sum_{\ell=-\infty}^{\infty}$$

$$A_{k\ell} \cos [2\pi (f_\ell k + f_f \ell) t + \phi_{k\ell}] \quad (31)$$

Equation 31 represents the general form of the video output as a function of time and has the added advantage that it defines the spectrum of  $v(t)$ . Inspection of Equation 31 shows that the components in the spectrum of  $v(t)$  are the line frequency harmonics with sidebands about them consisting of the frame frequencies. (see Figure 9) This should not be confused with the composite video frequency spectrum obtained previously, but rather this is the video spectrum before multiplication by the blanking signal.

The major advantage of expressing  $v(t)$  in the form of Equation 31 is that the coefficients,  $A_{k\ell}$ , which determine the spectrum of  $v(t)$  may be found directly from the image function,  $B(x,y)$ .

Using Equation 29,  $B(x,y)$  may be reduced to a cosine expression using the same method as for  $v(t)$ .  $B(x,y)$  then becomes

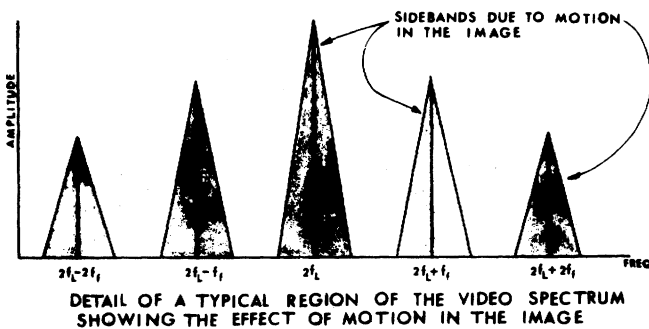
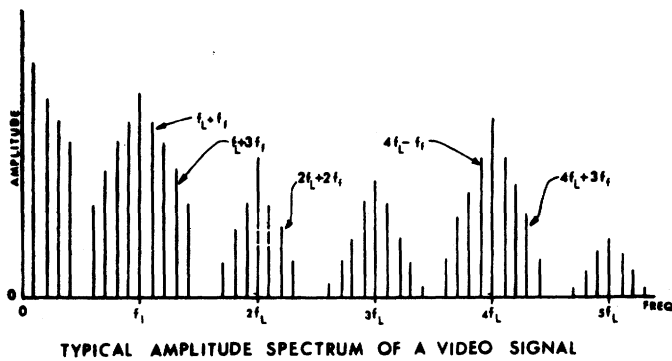


Figure 9

$$B(x,y) = \sum_{k=0}^{\infty} \sum_{l=-\infty}^{\infty}$$

$$[A_{k\ell} \cos \left( \frac{\pi k}{a} x + \frac{\pi l}{b} y \right) t + \phi_{k\ell}] \quad (32)$$

However, this expression is expandable by use of trig identities into

$$B(x,y) = \sum_{k=0}^{\infty} \sum_{l=-\infty}^{\infty} [a_{k\ell} \cos \left( \frac{\pi k}{a} x + \frac{\pi l}{b} y \right) + b_{k\ell} \sin \left( \frac{\pi k}{a} x + \frac{\pi l}{b} y \right)] \quad (33)$$

Where  $a_{k\ell} = A_{k\ell} \cos \phi_{k\ell}$

$$b_{k\ell} = A_{k\ell} \sin \phi_{k\ell}$$

It then follows by orthogonal relationships that

$$a_{pq} = \frac{1}{4ab} \int_0^{2a} \int_0^{2b}$$

$$B(x,y) \cos \left( \frac{\pi p}{a} x + \frac{\pi q}{b} y \right) dx dy \quad (34)$$

$$b_{pq} = \frac{1}{4ab} \int_0^{2a} \int_0^{2b}$$

$$B(x,y) \sin \left( \frac{\pi p}{a} x + \frac{\pi q}{b} y \right) dx dy \quad (35)$$

Then since  $A_{pq} = \sqrt{a_{pq}^2 + b_{pq}^2}$

the spectrum of  $v(t)$  is completely defined by evaluation of the integrals of Equation 34 and Equation 35.

#### General Aspects of the Spectrum of $v(t)$

There are several points of interest concerning the video spectrum which are brought to light by this approach. The first of these is that the process of scanning transforms each of the spacial Fourier components of  $B(x,y)$  into a component in the spectrum of  $v(t)$ . This transformation is made on a one to one basis and any nonlinearity in the scanning device which alters the amplitude of these components or generates new ones will produce distortion of the video signal.

Another item of interest is the effect of motion in the image. If the image is changing from one scan to another, then the effect this has on the Fourier series expansion of  $B(x,y)$  is to make the coefficients,  $A_{k\ell}$ , functions of time. Since these coefficients are also the coefficients in the Fourier series expansion of  $v(t)$ , each component of  $v(t)$  is of the form

$$A(t) = A_{k_1 l_1}(t) \cos$$

$$[(k_1 f_1 + l_1 f_f) 2\pi t + \phi_{k_1 l_1}] \quad (36)$$

Where  $A(t)$  is the amplitude of the  $k_1 \ell_1$  components.

Inspection of Equation 36 reveals that it is an exact expression for a double sideband suppressed carrier signal. The spectrum of each component of  $v(t)$  takes on sidebands with the maximum frequency of the sidebands equal to the maximum frequency of the motion in the image. Figure 9 is a blown-up portion of a part of such a spectrum of  $v(t)$ . Note that if the frequency of the motion is greater than  $1/2$  the frame frequency, aliasing will result, causing a blurring effect in the received image.

Another point of interest is the effect of scanning with a finite aperture. Up to this point in the discussion, the aperture through which the scanning device viewed the image has been assumed to be a point. If it is not a point but rather a small area with its response dependent upon the location of the image point in the area, then these results must be modified. The effect of such an aperture is to smooth the time series representing  $v(t)$  and thus to modify the spectrum much as a filter would. By extending this basic filter concept, Mertz and Gray [11] were able to show that a finite two dimensional aperture has the effect of a comb filter with its response peaks at the harmonics of the line frequency. Thus, the effect of a finite aperture on the spectrum is to further confine the components to bands of frequencies about the harmonics of the line frequency. (The convergence of the Fourier series expansion of  $v(t)$  also has the effect of confining the energy to these bands in the spectrum.)

One precaution which must be observed in using this method is that  $B(x,y)$  must truly be a function of both  $x$  and  $y$ . Otherwise, the integrals of Equations 34 and 35 are identically zero. However, this is not a fault of the theory, but rather a violation of one of its assumptions. It is tacitly assumed that the Fourier series for  $B(x,y_1)$  differs from that of  $B(x,y_2)$ . If  $B(x,y)$  is not a function of  $y$ , the theory collapses. However, when this condition exists, the situation is easily rectified

by expanding  $B(x)$  or  $B(y)$  in its corresponding one dimensional series.

#### Development of a Numerical Method for Approximating the Spectrum of $v(t)$

It is desirable to have a numerical technique for approximating the spectrum of  $v(t)$  in order to avoid evaluation of the integrals in Equation 34 and Equation 35. The reason for avoiding this integration is the difficulty of obtaining a mathematical expression for  $B(x,y)$  when the image is normal program material. In order to obtain such an approximation, it is sufficient to make  $x$  and  $y$  discrete and then find coefficients of the double Fourier series such that the series exactly represents  $B(x,y)$  at the discrete points in question. If  $x$  is allowed to take on  $2N$  values and  $y$  is allowed to take on  $2M$  values, then  $x$  and  $y$  become periodic in  $2N$  and  $2M$  respectively. Taking the new periods of  $x$  and  $y$  into account, Equation 26 may be re-written in an approximated form as

$$B(x,y) = \sum_{k=0}^{N-1} \sum_{\ell=0}^{M-1} [a_{k\ell} \cos \left( \frac{\pi k}{N} x + \frac{\pi \ell}{M} y \right) + b_{k\ell} \sin \left( \frac{\pi k}{N} x + \frac{\pi \ell}{M} y \right)] \quad (37)$$

Where  $b_{0,\ell} = b_{k,0} = 0$

The reasons for the limits on the summation will become clear as formulas for  $a_{k\ell}$  and  $b_{k\ell}$  are derived. The dropping of the negative values of  $\ell$  is possible because  $a_{k,\ell} = a_{k,-\ell}$  and  $b_{k\ell} = b_{k,-\ell}$ : i.e., the spectrum is symmetrical with respect to the line frequency harmonics.

Thus, the problem of expanding the Equation 37 to obtain the video spectrum resolves itself into the problem of obtaining  $a_{k\ell}$  and  $b_{k\ell}$  in a numerical form suitable for machine calculation. Before proceeding to the derivation of these coefficients, it is helpful to state three lemmas (see Appendix I) which are necessary in the derivation.

Lemma I

$$\sum_{x=0}^{2N-1} \sum_{y=0}^{2M-1} \sum_{k=0}^{N-1} \sum_{l=0}^{M-1} b_{k\ell} \sin \left( \frac{\pi k}{N} x + \frac{\pi l}{M} y \right) \cos \left( \frac{\pi p}{N} x + \frac{\pi q}{M} y \right) = 0$$

Lemma II

$$\sum_{x=0}^{2N-1} \sum_{y=0}^{2M-1} \sum_{k=0}^{N-1} \sum_{l=0}^{M-1} a_{k\ell} \cos \left( \frac{\pi k}{N} x + \frac{\pi l}{M} y \right) \cos \left( \frac{\pi p}{N} x + \frac{\pi q}{M} y \right) = 2a_{pq}^{MN}$$

$0 < q < M-1$   
 $0 < p < N-1$   
 $p$  and  $q$  not both zero

Lemma III

$$\sum_{x=0}^{2N-1} \sum_{y=0}^{2M-1} \sum_{k=0}^{N-1} \sum_{l=0}^{M-1} b_{k\ell} \sin \left( \frac{\pi k}{N} x + \frac{\pi l}{M} y \right) \sin \left( \frac{\pi p}{N} x + \frac{\pi q}{M} y \right) = 2MNb_{pq}$$

$0 < p < N-1$   
 $0 < q < M-1$

It is now possible to derive expressions for  $a_{pq}$  and  $b_{pq}$  as functions of  $B(x,y)$ . Multiplying both sides of Equation 37 by

$$\cos \left( \frac{\pi p}{N} x + \frac{\pi q}{M} y \right)$$

and summing over  $x$  and  $y$  yields

$$\sum_{x=0}^{2N-1} \sum_{y=0}^{2M-1} B(x,y) \cos \left( \frac{\pi p}{N} x + \frac{\pi q}{M} y \right) = \sum_x \sum_y \sum_k \sum_l a_{k\ell} \cos \left( \frac{\pi k}{N} x + \frac{\pi l}{M} y \right) \cos \left( \frac{\pi p}{N} x + \frac{\pi q}{M} y \right) + \sum_x \sum_y \sum_k \sum_l b_{k\ell} \sin \left( \frac{\pi k}{N} x + \frac{\pi l}{M} y \right) \cos \left( \frac{\pi p}{N} x + \frac{\pi q}{M} y \right) \quad (38)$$

Applying Lemma 2 to the first sum on the right-hand side of Equation 44 and Lemma 1 to the second sum of Equation 44 obtained to

$$\sum_{x=0}^{2N-1} \sum_{y=0}^{2M-1} B(x,y) \cos \left( \frac{\pi p}{N} x + \frac{\pi q}{M} y \right) = 2MN a_{pq} \quad (39)$$

By rearranging Equation 39, the desired expression for  $a_{pq}$  is obtained as

$$a_{pq} = \frac{1}{2NM} \sum_{x=0}^{2N-1} \sum_{y=0}^{2M-1} B(x,y) \cos \left( \frac{\pi p}{N} x + \frac{\pi q}{M} y \right) \quad \begin{matrix} 0 < p < N-1 \\ 0 < q < M-1 \\ p=q \neq 0 \end{matrix} \quad (40)$$



Similarly, multiplying Equation 37 through by

$$\sin\left(\frac{\pi p}{N}x + \frac{\pi q}{M}y\right)$$

and summing over x and y, the expression for  $b_{pq}$  is seen to be

$$b_{pq} = \frac{1}{2NM} \sum_{x=0}^{2N-1} \sum_{y=0}^{2M-1} B(x,y) \cos\left(\frac{\pi p}{N}x + \frac{\pi q}{M}y\right) \quad \begin{matrix} 0 < p < N-1 \\ 0 < q < M-1 \end{matrix} \quad (41)$$

Equations 40 and 41 are an approximation of the amplitude and phase spectrum of  $v(t)$  according to Equation 37. Also Equations 40 and 41 are in a form which may be used for machine computation, since their evaluation requires no more than arithmetical operations.

#### Description of the Computer Program to Find the Spectrum of $v(t)$

In order to use Equations 40 and 41 for machine computation, the brightness function  $B(x,y)$  must be specified at  $4MN$  points equally spaced over the image. In the program used on this project, this was done by forming  $B$  into a matrix and storing this matrix on tape. The values of  $M$  and  $N$  were taken as 150 each, thus yielding 90,000 data points over the image. These points are then read off the tape, and Equations 40 and 41 evaluated to give  $a_{pq}$  and  $b_{pq}$ . Since the amplitude spectrum is of primary interest the amplitude,

$$A_{pq} = \sqrt{a_{pq}^2 + b_{pq}^2}$$

is calculated and this is the result plotted in all the following spectrums. A copy of this program, as well as an example of the ones used to generate the  $B$  matrix, may be found in [13].

The first image which was selected for analysis was a white circle and

black background. This image was chosen for two reasons. The first was that it represents typical program material for the Apollo television system: i.e., such an image would be seen by astronauts as they approach the moon in their Apollo space capsule. Secondly, an exact analytical result for this image was given by Mertz and Gray in 1934 [11]. Table III is a comparison of the computer results with their analytical results.

Another example for which analytical results are available is the diagonal bar presented in Part II. Therefore, as a second check on the computer algorithm, this spectrum was investigated. The spectrum of the white bar placed at an angle of  $45^\circ$  with the x axis was analyzed using the computer routine. The results are presented in Figures 10, 11, and 12. Figure 10 is the spectrum of the line frequency harmonics and represents the over-all coarse spectrum. Observe that the envelope is very nearly the  $\sin x/x$  distribution of a single pulse produced by the scanning process as was predicted in Part II. Figures 11 and 12 are blown-up versions of Figure 10, showing the fine detail of the spectrum--both the low and the high frequency regions. The actual numbers are representative of the Apollo (mode 1) system. Observe that the spectrum is more diffused from the line frequency harmonics in the upper frequency regions, as was predicted for a non-vertical line in Part II.

#### Extension of Computer Model to the Composite Video Spectrum

Up to this point in this chapter, the spectrum under consideration has been the spectrum of the video signal only: i.e., without blanking and synchronization. Since in Part II the synchronization was shown to be an additive term resulting from a one dimensional series, neglecting this term represents a straight forward correction.

However, neglecting the blanking signals is a much more difficult item

TABLE III

P	Q	*ACTUAL FREQUENCY IN Hz	CALCULATED AMPLITUDE	#MERTZ AND GRAY'S AMPLITUDE	DIFFERENCE
1	0	3200	.152	.153	.001
1	1	3210	.131	.130	.001
1	2	3220	.079	.079	.000
1	3	3230	.023	.023	.000
1	4	3240	.014	.014	.000
2	0	6400	.094	.095	.001
2	1	6410	.079	.079	.000
2	2	6420	.042	.040	.002
2	3	6430	.0023	.0024	.0001
2	4	6440	.020	.021	.001
3	0	9600	.032	.032	.00
3	1	9610	.023	.023	.00
3	2	9620	.0023	.0024	.001
3	3	9630	.017	.017	.000
3	4	9640	.023	.023	.000
4	0	12800	.011	.012	.001
4	1	12810	.014	.014	.000
4	2	12820	.021	.021	.000
4	3	12830	.023	.023	.000
4	4	12840	.0169	.0168	.0001
5	0	16000	.023	.023	.000
6	0	19600	.0121	.0126	.0005
7	0	22800	.0041	.0047	.0006
8	0	26000	.0118	.0113	.0005
9	0	29200	.0065	.0061	.0004
10	0	32400	.0025	.0027	.0002
11	0	35600	.0072	.0071	.0001
12	0	38800	.0046	.0042	.0004
13	0	42000	.0014	.0019	.0005
14	0	45200	.0048	.0049	.0001

\* Frequency Calculation based on Apollo mode 1 scanning parameters

$$\# A_{pq} = \frac{R}{2ab} \left[ \frac{1}{\left(\frac{P}{2a}\right)^2 + \left(\frac{Q}{2b}\right)^2} \right]^{\frac{1}{2}} J_1 \left[ 2 R \sqrt{\left(\frac{P}{2a}\right)^2 + \left(\frac{Q}{2b}\right)^2} \right]$$

Where a = length of picture  
 b = height of picture  
 R = radius of circle  
 $J_1$  = first order bessel function

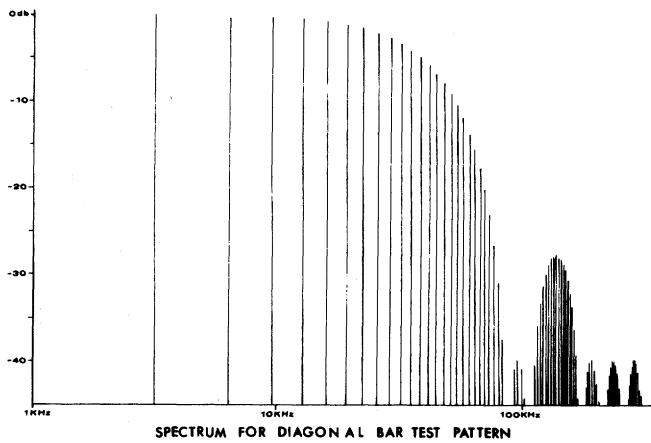


Figure 10

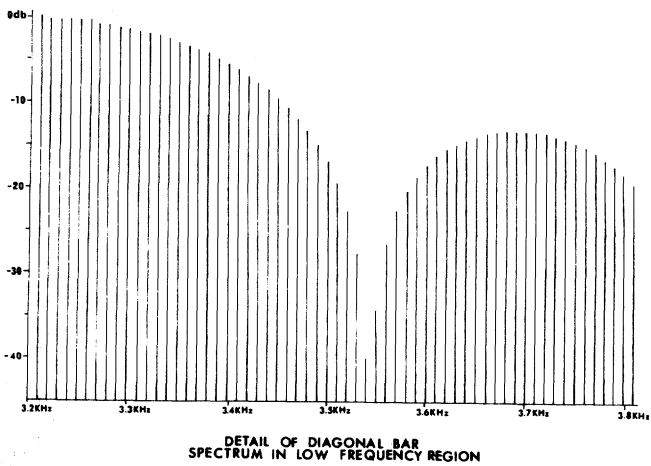


Figure 11

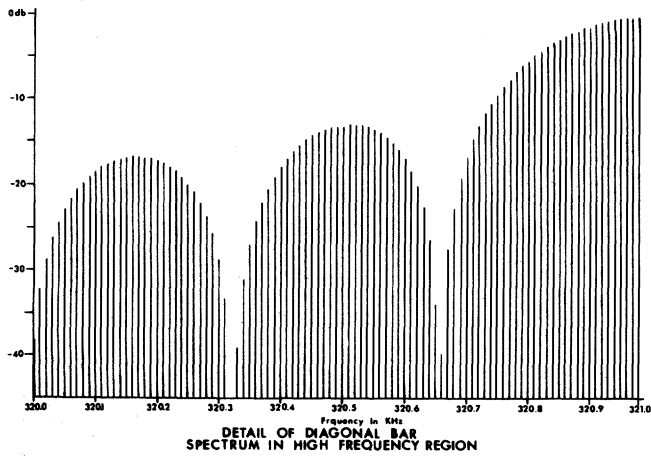


Figure 12

to correct, since the blanking functions are multiplying  $v(t)$ . Thus, if the model is to be of any real use, the blanking signals must be accounted for. With the computer algorithm already developed, the simplest method of adding the blanking is to put it into  $B(x,y)$ . This may be accomplished by placing a strip of zero brightness along the top of the image to represent vertical blanking and by placing a strip of zero brightness along the right hand edge to represent horizontal blanking. This argument is illustrated in Figure 13 and the resulting  $v(t)$  is sketched.

With this simple extension, the computer algorithm presented in the last section yields the composite video spectrum generated by transmitting any monochrome image. In the examples close observation will reveal that the nulls in the calculated spectrums are slightly shifted from those measured by NASA. The reason for this is the different ratios of the  $T/t$ . NASA's ratio was .0965 while the best approximation to this which can be made using the previously mentioned 300 by 300 grid is .100.

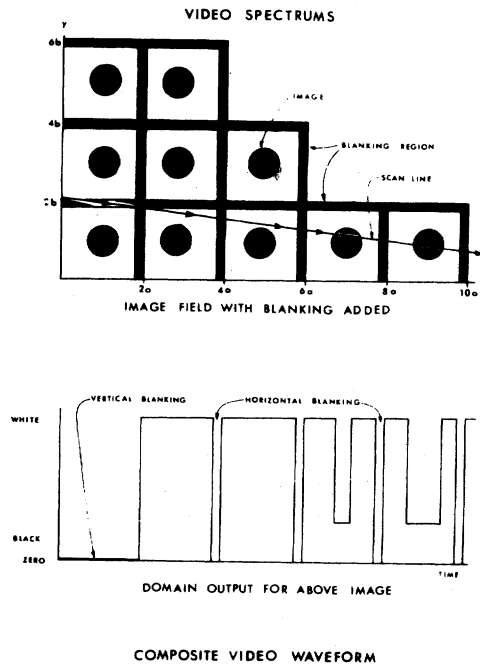


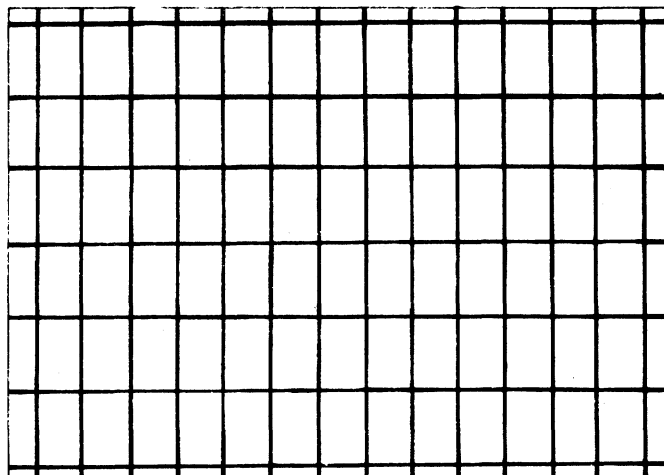
Figure 13

Composite Video Spectrums of Some Standard Test Patterns

With the model extended to the composite video spectrum, it is now feasible to determine spectrums of standard television test patterns. The ones selected for this study are representative of those used by NASA engineers for testing the Apollo system.

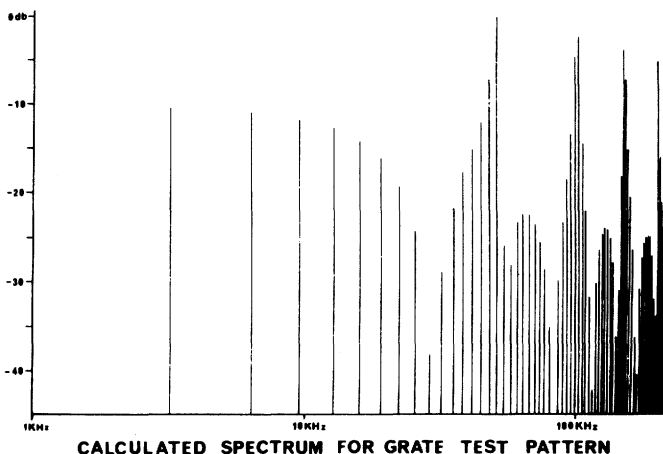
Knowing the theoretical spectrum of standard test patterns is important to television engineers for two reasons--one being to insure the test pattern is actually testing the parameter of the system which it is designed to test, and secondly, to compare with experimental test data to evaluate system performance. The pattern selected for this work to demonstrate the use of the model is the grate scale pattern shown in Figure 14. The contrast ratio is 100, and the plots of the spectrum are made using mode 1 Apollo scan parameters. The composite video spectrum produced by the grate pattern has been plotted in Figure 15. Figure 16 is a measured reproduction of the spectrum. The agreement is seen to be quite good in general, with the major difference being in the large peak at 50 KHz which the computer algorithm predicted but was not published in the measured results. However, the peaks at 100 KHz, 150 KHz, 200 KHz, and up do agree. The fact that a peak was measured at 100 KHz and at intervals of 50 KHz thereafter indicates that these peaks are being generated by a 50 KHz fundamental and its harmonics. Thus, it would seem that the algorithm is correct and the lack of this large 50 KHz peak may represent an oversight in the measured spectrum.

An interesting phenomenon was observed in calculating this spectrum. The contrast ratio first used was infinite, then changed to 1000, and finally changed to 100. As this ratio was decreased, the peaks of the spectrum were lower and the level of the valleys raised. This phenomenon apparently has not been observed by other workers in this area and needs experimental verification to prove or disprove that the contrast ratio has an effect on the composite video spectrum.



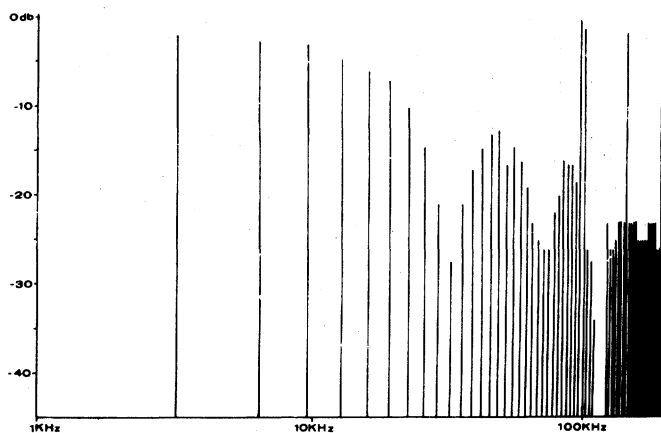
GRATE PATTERN  
NASA TEST PATTERN

Figure 14



CALCULATED SPECTRUM FOR GRATE TEST PATTERN

Figure 15



MEASURED SPECTRUM FOR GRATE TEST PATTERN

Figure 16

## CONCLUSION

A mathematical model for a deterministic composite video signal has been presented and the resulting spectrum examined. The most difficult problem involved in using the model was obtaining the spectrum of the scanned video signal. This problem was solved by applying the methods of numerical analysis to the theory of scanning developed by Mertz and Gray and extending this theory to include blanking. The resulting computer program will obtain the composite video spectrum resulting from scanning any general image.

Obtaining the spectrum of the composite video signal was only half of the problem, however. The related problem of specifying the necessary bandwidth for a television system was discussed. The conclusions concerning bandwidth which may be drawn are twofold. First, if the program material which the television system must transmit is known, then the methods of this work may be applied to this material and the resulting spectrums will determine the necessary system bandwidth. The bandwidth determined in this manner will be a much better approximation than any of the methods presented in Part I. For example, if the only image to be transmitted is the half black and half white test pattern examined in Part II, then the necessary system bandwidth would be on the order 100 KHz. (Assuming Apollo mode 1 scan parameters) This is approximately one-fourth of the bandwidth predicted by any of the methods in Part I. However, if the only specification concerning the bandwidth available is the maximum horizontal resolution, then the standard methods presented in Part I yield good estimations of the maximum bandwidth. Even in this case, it is feasible to use the methods of this work on probable images and let the results serve as a check on the standard methods.

An extension of this work to random video processes would relieve the burden of knowing the exact images to be transmitted. L. E. Franks of Bell Telephone Laboratories has published a paper in this area. [9]

## Appendix 1:

A proof is herein derived for the first of the lemmas used in the text. The remaining proofs are similar and are derived in a report prepared for NASA [13].

### Lemma I

$$\sum_{x=0}^{2N-1} \sum_{y=0}^{2M-1} \sum_{k=0}^{N-1} \sum_{\ell=0}^{M-1} b_{k\ell} \sin \left( \frac{\pi k}{N} x + \frac{\pi \ell}{M} y \right) \cos \left( \frac{\pi p}{N} x + \frac{\pi q}{M} y \right) = 0$$

Proof:

$$S = \sum_x \sum_y \sum_k \sum_\ell b_{k\ell} \sin \left( \frac{\pi k}{N} x + \frac{\pi \ell}{M} y \right) \cos \left( \frac{\pi p}{N} x + \frac{\pi q}{M} y \right)$$

Expanding by trig. identities

$$S = \sum_x \sum_y \sum_k \sum_\ell b_{k\ell} \left( \sin \frac{\pi k}{N} x \cos \frac{\pi \ell}{M} y + \cos \frac{\pi k}{N} x \sin \frac{\pi \ell}{M} y \right) \left( \cos \frac{\pi p}{N} x \sin \frac{\pi q}{M} y - \sin \frac{\pi p}{N} x \sin \frac{\pi q}{M} y \right)$$

Carrying out the indicated multiplication

$$S = \sum_x \sum_y \sum_k \sum_\ell b_{k\ell} \sin \frac{\pi k}{N} x \cos \frac{\pi \ell}{M} y \cos \frac{\pi p}{N} x \cos \frac{\pi q}{M} y -$$

$$\sum_x \sum_y \sum_k \sum_\ell b_{k\ell} \sin \frac{\pi k}{N} x \sin \frac{\pi p}{N} x \cos \frac{\pi \ell}{M} y \sin \frac{\pi q}{M} y +$$

$$\sum_x \sum_y \sum_k \sum_\ell b_{k\ell} \cos \frac{\pi k}{N} x \sin \frac{\pi p}{M} y \cos \frac{\pi p}{N} x \cos \frac{\pi q}{M} y -$$

$$\sum_x \sum_y \sum_k \sum_\ell b_{k\ell} \cos \frac{\pi k}{N} x \sin \frac{\pi \ell}{M} y \sin \frac{\pi p}{N} x \sin \frac{\pi q}{M} y$$

and by rearranging

$$S = \sum_{y=0}^{2M-1} \sum_{k=0}^{N-1} \sum_{\ell=0}^{M-1} b_{k\ell} \cos \frac{\pi \ell}{M} y \cos \frac{\pi q}{M} y \sum_{x=0}^{2N-1} \sin \frac{\pi k}{N} x \cos \frac{\pi p}{N} x -$$

$$\sum_{x=0}^{2N-1} \sum_{k=0}^{M-1} \sum_{\ell=0}^{M-1} b_{k\ell} \sin \frac{\pi k}{N} x \sin \frac{\pi p}{N} x \sum_{y=0}^{2M-1} \cos \frac{\pi \ell}{M} y \sin \frac{\pi q}{M} y +$$

$$\sum_{x=0}^{2N-1} \sum_{k=0}^{N-1} \sum_{\ell=0}^{M-1} b_{k\ell} \cos \frac{\pi k}{N} x \cos \frac{\pi p}{N} x \sum_{y=0}^{2M-1} \cos \frac{\pi q}{M} y \sin \frac{\pi \ell}{M} y -$$

$$\sum_{y=0}^{2M-1} \sum_{k=0}^{N-1} \sum_{\ell=0}^{M-1} b_{k\ell} \sin \frac{\pi \ell}{M} y \sin \frac{\pi q}{M} y$$

$$\sum_{x=0}^{2N-1} \sin \frac{\pi p}{N} x \cos \frac{\pi k}{N} x$$

but it is known that (12)

$$\sum_{z=0}^{2i-1} \sin \frac{\pi}{i} jz \cos \frac{\pi}{i} hz = 0 \quad (A)$$

Thus applying this theorem to each of the single series above S becomes, S = 0

QED

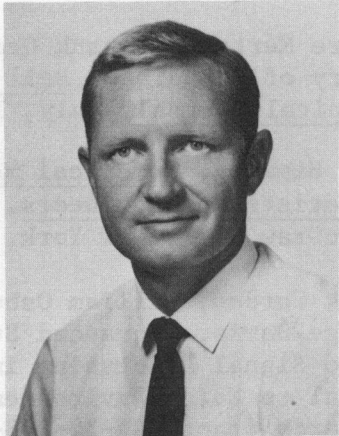
#### REFERENCES

1. Stanley Lebar and Charles Hoffman, "TV Show of the Century", Electronics, March 6, 1967.
2. R.C. Brainard, "Subjective Evaluation of PCM Noise-Feedback Coder for Television", Proceedings of I.E.E.E., March, 1967.
3. W.W. Harman, Principles of the Statistical Theory of Communications, McGraw Hill, New York, 1961, pp. 115-116.
4. John Hancock, The Principles of Communication Theory, McGraw Hill, New York, 1961, pp. 175-176.

5. V.K. Zworykin and G.A. Morton, Television, John Wiley & Sons, Inc., New York, 1954, pp. 184-185.
6. Glenn M. Glasford, Fundamentals of Television Engineering, McGraw Hill, New York, 1955, Chapter 2.
7. Jacob Millman and Herbert Taub, Pulse and Digital Circuits, McGraw Hill, New York, 1956, p. 66.
8. Harold A. Wheeler and Authur V. Loughren, "Fine Structure of Television Images", Proceedings of I.R.E. May, 1938.
9. L.E. Franks, "A Model for the Random Video Process", Bell System Technical Journal, April, 1966.
10. J.B. Chatten, R.G. Clapp, and D.G. Fink, "The Composite Video Signal -- Waveforms and Spectrum", I.R.E. Transactions on Broadcast and Television Receivers, July, 1955.
11. Pierre Mertz and Frank Gray, "A Theory of Scanning", Bell System Technical Journal, July, 1934.
12. R.W. Hamming, Numerical Methods for Scientists and Engineers, Chapter 6, McGraw Hill, New York, 1962.
13. Frank Carden, William Osborne, and George Davis, "Advanced Study of Video Signal Processing in Low Signal to Noise Environments", NASA Research Grant NGR-32-003-037. A Report by Engineering Experiment Station, New Mexico State University, December, 1967.

## BIOGRAPHIES

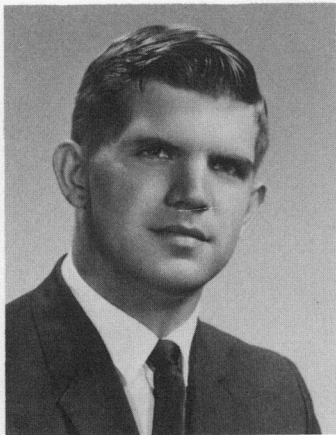
Frank F. Carden was born in Abilene, Texas on March 15, 1932. He received his B.S. degree in Electrical Engineering from Lamar State College of Technology, Beaumont, Texas in 1959, and he received the Ph.D. from Oklahoma State University, Stillwater, Oklahoma in 1965.



Mr. Carden has worked as a research engineer at Texas Instruments in the area of anti-radiation missile, and he has worked for NASA as a NASA-ASEE summer fellow.

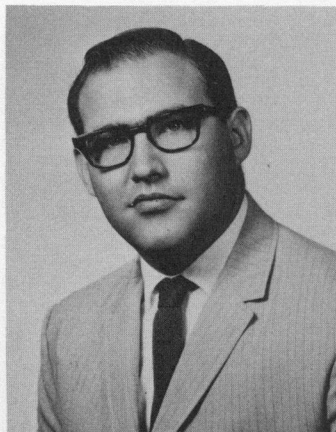
He is currently Professor and Head of the Electrical Engineering Department at New Mexico State University and the director of the Communication Research Group in the Electrical Engineering Department. Mr. Carden is a consultant for White Sands Missile Range in the area of communication systems.

Dr. Carden is a member of Eta Kappa Nu and IEEE.



Alton L. Gilbert (S'68) was born in Elmira, New York on April 13, 1942. He received the B.S.E.E. degree (with high honors) from New Mexico State University in 1970. Since June 1969 he has been associated with the Communications Research Group at New Mexico State University, and has undertaken research in communications with two previous papers published in this area. He is the 1970-71 IEEE Fortescue Fellow and is doing graduate work at New Mexico State University.

Mr. Gilbert is a member of Sigma Xi, Phi Kappa Phi, Eta Kappa Nu, and Sigma Tau.



William P. Osborne (S'65-M'70) was born in Benton, Kentucky on February 2, 1944. He received the B.S.E.E. and M.S.E.E. degrees from the University of Kentucky, Lexington, Kentucky in 1966 and 1968 respectively, and the Sc.D. degree from New Mexico State University, Las Cruces, New Mexico in 1970.

During the summer of 1966, he worked for Collins Radio Company in Cedar Rapids, Iowa. From 1967 to 1970, he was employed by the Communications Research Group at New Mexico State University. Since January of 1970, he has been employed with the Systems Division of Radiation, Inc., in Melbourne, Florida. His principal interests are in stochastic systems.

Dr. Osborne is a member of Eta Kappa Nu and Sigma Xi.